LETTER

https://doi.org/10.1038/s41586-018-0191-2

Parallel emergence of stable and dynamic memory engrams in the hippocampus

Thomas Hainmueller[1,2,3] & Marlene Bartos[1]*

During our daily life, we depend on memories of past experiences to plan future behaviour. These memories are represented by the activity of specific neuronal groups or 'engrams'[1,2]. Neuronal engrams are assembled during learning by synaptic modification, and engram reactivation represents the memorized experience[1]. Engrams of conscious memories are initially stored in the hippocampus for several days and then transferred to cortical areas[2]. In the dentate gyrus of the hippocampus, granule cells transform rich inputs from the entorhinal cortex into a sparse output, which is forwarded to the highly interconnected pyramidal cell network in hippocampal area CA3[3]. This process is thought to support pattern separation[4] (but see refs. [5,6]). CA3 pyramidal neurons project to CA1, the hippocampal output region. Consistent with the idea of transient memory storage in the hippocampus, engrams in CA1 and CA2 do not stabilize over time[7–10]. Nevertheless, reactivation of engrams in the dentate gyrus can induce recall of artificial memories even after weeks[2]. Reconciliation of this apparent paradox will require recordings from dentate gyrus granule cells throughout learning, which has so far not been performed for more than a single day[6,11,12]. Here, we use chronic two-photon calcium imaging in head-fixed mice performing a multiple-day spatial memory task in a virtual environment to record neuronal activity in all major hippocampal subfields. Whereas pyramidal neurons in CA1–CA3 show precise and highly context-specific, but continuously changing, representations of the learned spatial sceneries in our behavioural paradigm, granule cells in the dentate gyrus have a spatial code that is stable over many days, with low place- or context-specificity. Our results suggest that synaptic weights along the hippocampal trisynaptic loop are constantly reassigned to support the formation of dynamic representations in downstream hippocampal areas based on a stable code provided by the dentate gyrus.

To study hippocampal memory engrams during long-term learning, we designed a goal-oriented learning task for head-fixed mice. Mice ran on a spherical treadmill to collect soy milk rewards on a 4-m-long virtual linear track displayed on monitors around the animal. After at least 10 days of familiarization to this track (familiar context), imaging sessions started in which mice ran alternatingly on this familiar and a visually different, novel track with different reward sites (Fig. 1a, b, Supplementary Video 1). Animals consistently licked more often inside than outside reward zones on both tracks (Fig. 1d). Initially, overall licking and reward-related licking were lower in the novel context than in the familiar context (Extended Data Fig. 1c, d). These differences vanished with learning. On the novel track, the ratio of rewarded to erroneous licks increased markedly on the second training day (Fig. 1d), indicating that mice remembered the rewarded locations.

To measure hippocampal neuronal activity, mice were injected with adeno-associated viruses designed to express the fluorescent calcium indicator GCaMP6f pan-neuronally in CA1 and the dentate gyrus (DG) or CA3 (Fig. 1c). A chronic transcortical imaging window was implanted above CA1 to perform two-photon imaging of CA1 or DG neurons[13] (Supplementary Video 2). Implantation did not impair spatial learning in a Barnes maze (Extended Data Fig. 1h, i). CA1 and DG neurons were imaged at depths of around 150 μm and around 700 μm, respectively. To image CA3, we

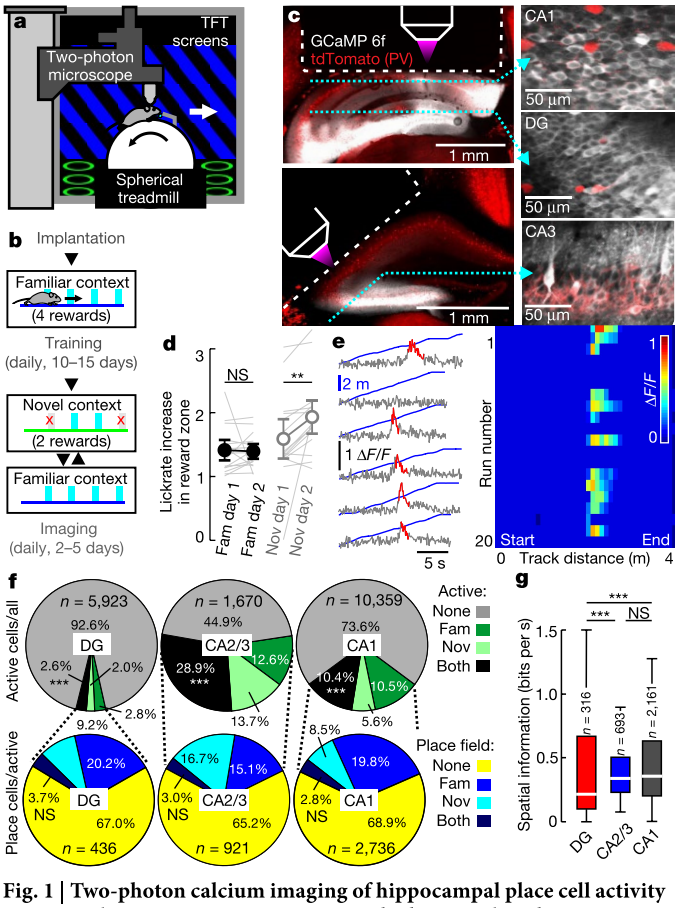

Fig. 1 | Two-photon calcium imaging of hippocampal place cell activity in a virtual environment. a, Experimental schematic. **b**, Behaviour timeline (see Methods). **c**, Left, CA1 and DG (top) and CA2/3 (bottom) implantation sites. GCaMP6f (white) and td-Tomato (tdT; red) in parvalbumin (PV)-expressing interneurons. Dotted lines, imaging planes. Right, GCaMP6f and tdT fluorescence in vivo. **d**, Ratio between rewarded and non-rewarded licks in the familiar (fam, filled circles) and novel (nov, open circles) contexts ($n = 15$ mice; two-sided signed rank-sum test). **e**, Calcium traces (grey) with significant transients (red; see Methods) of a GC and linear-track position (blue) over time. Right, calcium activity over track distance of the same GC. **f**, Top, fraction of active (more than 0.05 transients per s) cells among all neurons. Test for population overlap (χ^2 test). Bottom, cells with place fields among active cells. **g**, Spatial information for all familiar-track-active neurons (ANOVA on ranks, Dunn's test). Boxes, 25th to 75th percentiles; bars, median; whiskers, 99% range. NS, not significant; $^{***}P < 0.001$. Error bars denote s.e.m. For exact P values see Supplementary Table 1.

[1]Institute for Physiology I, Systemic and Cellular Neurophysiology, University of Freiburg, Freiburg, Germany. [2]Spemann Graduate School of Biology and Medicine (SGBM), University of Freiburg, Freiburg, Germany. [3]Faculty of Biology, University of Freiburg, Freiburg, Germany. *e-mail: marlene.bartos@physiologie.uni-freiburg.de

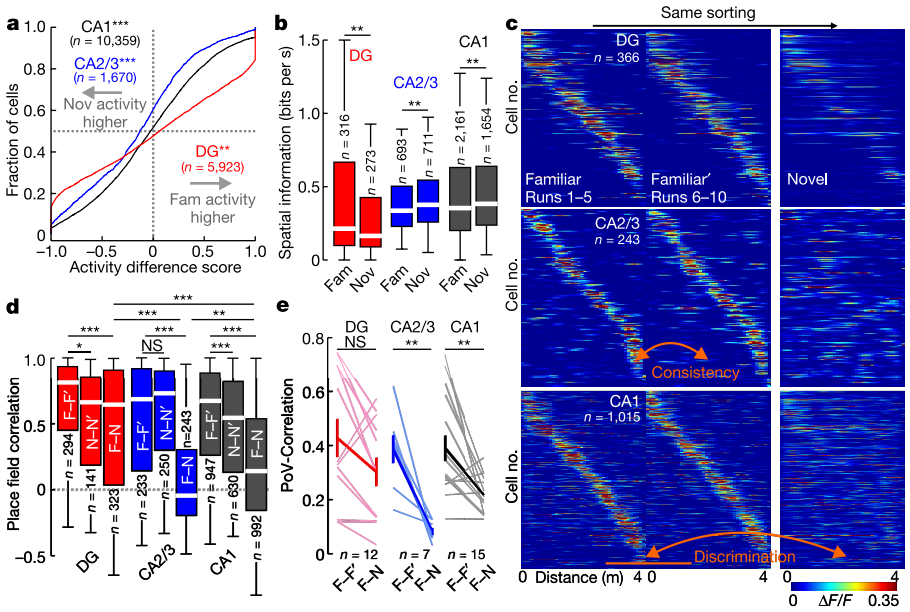

Fig. 2 | Pyramidal cells in CA1 and CA2/3 discriminate between contexts. a, Activity difference scores (see Methods) between novel and familiar contexts for all cells (two-sided signed rank-sum test: novel versus familiar activity). **b**, Mean spatial information of active cells (two-sided rank-sum test). **c**, Familiar-track place cell activity plotted for the first (left) and second (middle) block of familiar-context runs and for the novel context (right). **d**, Mean activity correlations of place cells within familiar (left) and novel context (middle) runs and between contexts (right bars; ANOVA on ranks, Dunn's test). **e**, PoV correlations (see Methods) for all experiments within familiar-context runs and between contexts (thin lines). Thick lines denote mean ± s.e.m. (two-sided paired *t*-test). Boxes, 25th to 75th percentiles; bars, median; whiskers, 99% range. $*P<0.05$, $**P<0.01$, $***P<0.001$; NS, not significant. For exact *P* values see Supplementary Table 1.

implanted a more lateral window[14] (Fig. 1c). Data were obtained predominantly from CA3 (Extended Data Fig. 2d), but some CA2 cells may also have been included[14]. In all cases, we used fast volumetric scanning to simultaneously record about 500 neurons (see Methods, Supplementary Videos 3–5).

We first analysed neuronal activity in the familiar and novel contexts (Fig. 1). Consistent with previous findings[11,12,15,16], pyramidal cells (PYRs) in CA1–CA3 were substantially more active than granule cells (GCs) (Fig. 1f, Extended Data Fig. 3a, b). We also determined the fraction of cells that was active in the familiar, novel or both contexts with more than 0.05 calcium transients per second. Activation of hippocampal neurons might be predetermined by intrinsic properties[17]. In line with this idea, we found a marked overlap of active neuronal ensembles between contexts (Fig. 1f, upper row). About 35% of these active neurons had a clearly defined place field (see Methods) on the first recording day in either the novel or the familiar context, or both (Fig. 1f, lower row). Because many neurons were active in both contexts, we investigated whether active neurons were more likely to have a place field in both contexts. However, the familiar- and novel-context place cells appeared to form independent subgroups within the active cell population (Fig. 1f, lower row) indicating that a separate place-coding group or 'engram' might exist for each context. Further comparison of spatial coding properties revealed lower average spatial information (see Methods) per active cell (Fig. 1g) and wider place fields (Extended Data Fig. 3c) in GCs compared to CA1–3 PYRs. Thus, GC activity is sparse and has broader and less precise spatial tuning than PYR activity.

Next, we compared neuronal activity between contexts (Fig. 2). Consistent with a previous study[15] and their inputs from the entorhinal cortex[18], mean activity in GCs decreased in the novel context, whereas mean activity of CA1 and CA2/3 PYRs increased (Fig. 2a). Similarly, novel-context spatial information was markedly lower in the DG, but higher in both CA regions (Fig. 2b). Additionally, there was a trend towards higher place cell numbers on the familiar track than on the novel track, particularly in the DG ($n=30.50$ versus 16.42 place cells per experiment, 12 experiments, $P=0.066$, paired *t*-test; Extended Data Fig. 3f). We next investigated the cause of these activity differences between contexts. Hippocampal γ-aminobutyric acid (GABA) interneurons contribute to separation of memory engrams[19] and formation of place fields[13]. We therefore analysed the activity of parvalbumin (PV)-expressing interneurons (PVIs; Extended Data Fig. 4), the most abundant subtype of interneurons in the hippocampus. PVI activity in CA1 and the DG correlated positively with running speed[13,20] (Extended Data Fig. 4c–h). PVIs in the DG, but not in CA1, showed decreased activity in the novel context (Extended Data Fig. 4i–l), contrasting with reports from unidentified DG interneurons[15]. Thus, our data argue against suppression of GCs by enhanced PVI activity, and are instead consistent with predominant recruitment of DG PVIs by local GC inputs.

To probe neuronal discrimination between contexts, we first determined the consistency of place cell firing on the same track between the first vs. the second block of five consecutive runs. Place cell consistency in the familiar context was high in all hippocampal subfields (Fig. 2c, d; F–F′). The same measure and trial-to-trial reliability were generally lower for novel-context runs, indicating an initially less reliable representation (Fig. 2c, d; N–N′; Extended Data Fig. 3i). Next, we quantified place cell remapping between the familiar and novel contexts. Unexpectedly, activity map correlations between contexts were substantially higher for DG place cells than in CA1 and CA2/3 (Fig. 2c, d; F–N). We confirmed this finding separately in two mice by imaging neuronal activity in CA1 and DG of the same mice (Extended Data Fig. 5). Thus DG place cell activity was similar between contexts, while that of CA1–3 place cells was highly discriminative. We also calculated population vectors (PoVs) for both contexts from the mean calcium activity maps of all cells. PoVs were significantly more dissimilar between contexts as compared to independent runs within the familiar context in CA1 and CA2/3 ($P=0.004$, both regions, paired *t*-test), but not in the DG ($P=0.051$, Fig. 2e). Indeed, activity map correlations between contexts were markedly lower in CA1 and CA2/3 than in the DG, indicating stronger remapping in CA1–3. GCs might encode travelled distance and therefore show low context-selectivity. To test this possibility, we let mice run on a simplified linear track with striped walls but no further contextual information (Extended Data Fig. 6a). Under these conditions, GC activity and spatial information were low, and GCs did not show consistent place fields (Extended Data Fig. 6b, c),

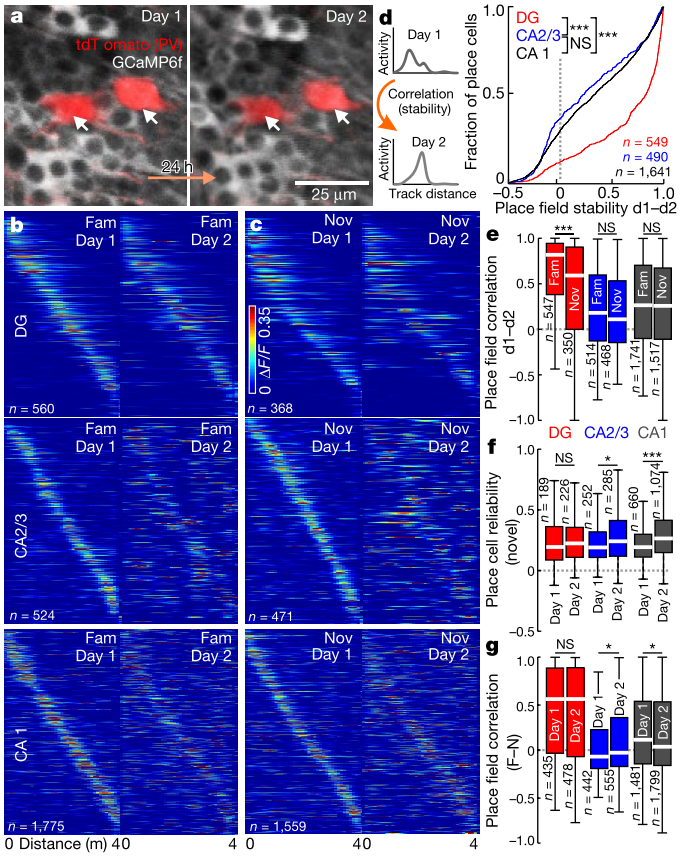

Fig. 3 | GC place fields are highly stable across days. a, Illustrative example of CA1 cells imaged on subsequent days. **b**, Activity of familiar-track place cells sorted for day 1. **c**, As in **b** for novel-track place cells. **d**, Left, experimental schematic. Right, activity map correlations between days for all day 1 (d1) place cells (ANOVA on ranks, Dunn's test). **e**, Activity map correlations between days for familiar-context (left) and novel-context (right) place cells. **f**, Mean trial-to-trial reliability of novel-track place cell responses on days 1 and 2. **g**, Activity map correlations between contexts of day 1 (left) and day 2 (right) place cells. **e–g**, Two-sided rank-sum test. Boxes, 25th to 75th percentiles; bars, median; whiskers, 99% range. $*P < 0.05$, $***P < 0.001$; NS, not significant. For exact P values see Supplementary Table 1.

indicating that they encode the general task layout rather than mere distance. Thus, GCs show reliable place representations and low context discrimination, whereas CA2/3 PYRs and CA1 PYRs prominently encode contextual differences.

To investigate place field stability throughout learning, we imaged the same cells in both contexts on two subsequent days (Fig. 3, Extended Data Fig. 7). Whereas GCs maintained their place field locations in the same context, CA1 PYRs and CA2/3 PYRs displayed substantial remapping (Fig. 3b–d). This was characterized by lower activity map correlations (Fig. 3d, e) and larger shifts of the preferred firing location (Extended Data Fig. 7c). Despite the generally high GC place field stability, activity map correlations between days were lower for GCs encoding the novel context than for those encoding the familiar context. By contrast, hippocampal PYRs showed similarly low stability in both contexts (Fig. 3e). Thus, GCs have stable place fields, while place fields in other hippocampal subfields change over days.

Place cell stability in CA1 may depend on environmental complexity[9]. We therefore repeated our experiments in a virtual context without distal visual cues ('poor') and a highly enriched, multisensory track ('rich'; Supplementary Video 6). Notably, the number of place cells was similar between all tracks, but their firing rate, spatial information and day-to-day stability were markedly reduced on the 'poor' track (Extended Data Fig. 8). We observed no differences between the 'rich' track and our standard contexts, indicating that CA1 place cell representations are also dynamic over days in complex environments.

Next, we investigated learning-induced changes in spatial coding. From day 1 to day 2, there was a substantial increase in the trial-to-trial reliability of place cells in CA1–3, but not in the DG (Fig. 3f, Extended Data Fig. 7d). The DG is required for context discrimination[5,6]. We therefore tested whether neuronal activity became more distinct between contexts with learning. Unexpectedly, activity correlations between contexts were unchanged in GCs from day 1 to day 2 but were lower for CA1 place cells on day 2 and remained negative in CA2/3 (Fig. 3g). Thus, improved behavioural context discrimination was accompanied by a decorrelation of place cell activity in CA1, but not in the DG.

In light of recent findings[20], we compared place coding between the deep and superficial sublayers of CA1. Notably, place field stability across days was slightly higher in deep-layer PYRs (45% difference, $P = 0.046$; Extended Data Fig. 9i), albeit at generally low levels. Place field reliability and context discrimination were comparable between sublayers (Extended Data Fig. 9g, h).

To investigate the development of spatial representations over the time-course of hippocampus-dependent memory[2], we continued imaging sessions for five subsequent days (Fig. 4, Extended Data Fig. 10). Whereas the number of place cells was similar for each context and day (Fig. 4c, white numbers), their firing locations changed markedly in some hippocampal sub-areas. Familiar-context place fields of GCs remained stable throughout all days (Fig. 4a–c) and novel-context place cells showed gradually increasing stability (Fig. 4b, c, Extended Data Fig. 10b). By contrast, CA1 and CA2/3 activity in the same contexts became rapidly more dissimilar over days. For CA2/3 cells, activity map correlations over more than two days dropped below chance levels (Fig. 4d), demonstrating that these neurons constantly remap their place fields.

Dynamic coding has been described in CA1[7–9,21], CA2[10] and other associative areas[22,23]. A gradual variation of active CA1 ensembles links contextual memories acquired close in time[7,8,21] and remapping of individual PYRs is driven by synaptic plasticity[13,24]. By contrast, neuronal ensemble activity in motor areas stabilizes throughout learning[25]. In the hippocampus, temporally stable coding of GCs may induce heterosynaptic plasticity at CA3 PYR dendrites by associating their activity with temporally dynamic inputs from the entorhinal cortex[23] or other CA3 PYRs[26]. This hypothesis would explain why CA3 ensembles can trigger memory recall independent of GC input even when the DG is required for initial task learning[27,28]. Our results, together with previous findings[8,10], indicate that CA3 coding can be dynamic or stable, potentially depending on the behaviour, proximo-distal location within CA3 (Extended Data Fig. 2e), virtual versus real-world navigation or species-differences in entorhinal cortex innervation[29]. When CA3 is stable, a mechanism similar to that described above may apply at CA3–CA1 synapses.

Traditionally, similar memories are thought to be represented by largely non-overlapping populations of GCs[4]. However, recent findings indicate that GCs remap only between widely dissimilar environments[11], while other cell types (for example, mossy cells) discriminate between similar contexts[12]. Accordingly, CA2/3 PYR activity was most discriminative between our virtual contexts (Fig. 2d, e). The high similarity of our—mostly mature[6]—GC activity between contexts may explain why mature GCs mediate generalization between similar contexts rather than pattern separation[5].

Our results further suggest that the hippocampus combines stable and dynamic coding and reunites findings of temporally varying neuronal ensembles encoding the same environment[7,8] with reports of stable behavioural output upon DG engram reactivation over weeks[2,27]. Given that the DG is required for the extinction or modification of existing memories acquired in the same scenery[28,30], our data support the hypothesis that GCs provide a simplistic but stable representation of the global environment[11,12] that serves as a blueprint for spatially and contextually precise, but temporally varying, CA1–3 engrams

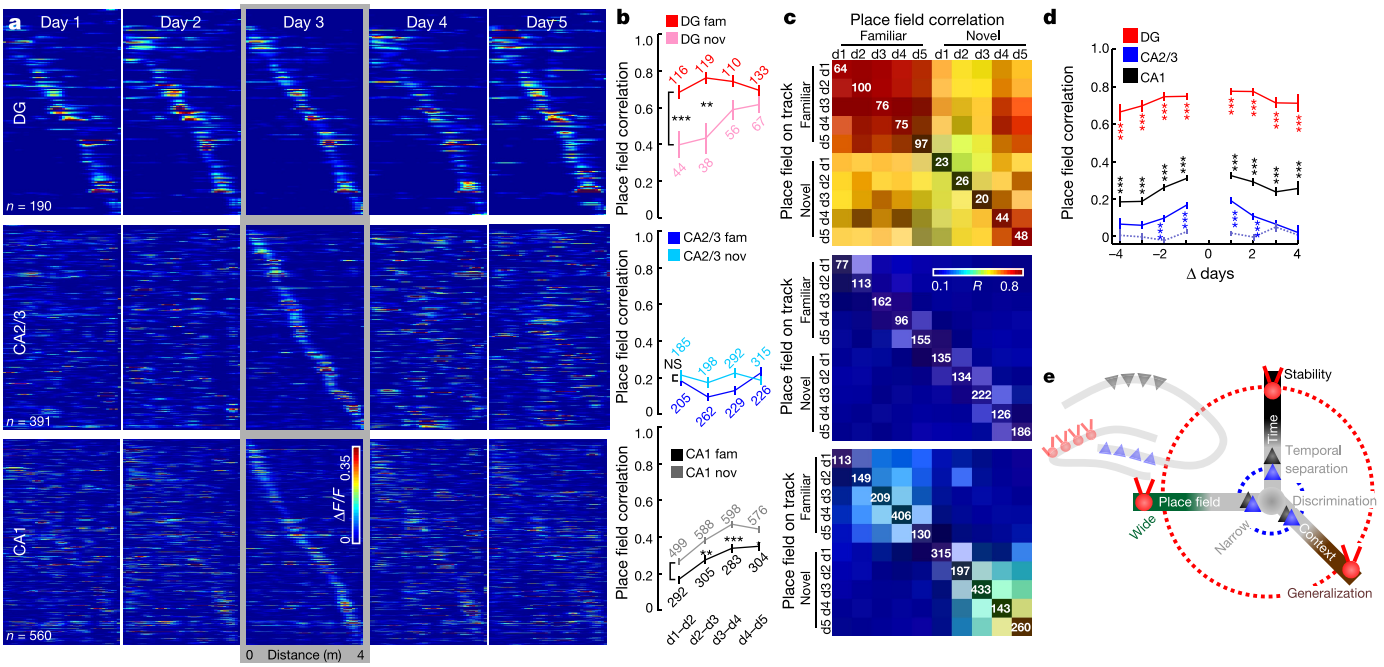

Fig. 4 | Stable coding of GCs persists throughout multiple days, whereas CA2/3 PYRs constantly remap over time. a, Activity maps of all familiar-context place cells sorted by day 3. **b**, Development of activity map correlations between subsequent days for familiar- (dark) and novel-context (light) place cells (numbers show *n*; ANOVA on ranks, Dunn's test; mean ± s.e.m.). **c**, Mean activity map correlations (colour coded; Pearson's *R*) over 5 days and two contexts as indicated on the *x*-axis. Each row shows mean correlation values for cells that had a place field on the day and track indicated on the *y*-axis (white numbers show *n*). **d**, Mean activity map correlations for familiar-context place cells over days passed. Grey dotted line, chance level correlations for CA2/3 cells obtained by shuffling cell IDs (two-sided rank-sum test, actual versus shuffled correlations, Bonferroni correction; mean ± s.e.m.). **e**, Schematic: GCs show a highly stable environment representation with low spatial and context selectivity. By contrast, PYRs form highly context-, place- and time-specific ensembles. $*P < 0.05$; $**P < 0.01$; $***P < 0.001$. For exact *P* and *n* values in **d** see Supplementary Table 1.

(Fig. 4e). Such an encoding scheme would allow one to associate memories acquired in the same global environment but still to discriminate between slightly different or temporally separate instances of these memories.

Online content

Any Methods, including any statements of data availability and Nature Research reporting summaries, along with any additional references and Source Data files, are available in the online version of the paper at https://doi.org/10.1038/s41586-018-0191-2.

Received: 20 November 2017; Accepted: 30 April 2018;

1. Ramirez, S. et al. Creating a false memory in the hippocampus. *Science* **341**, 387–391 (2013).
2. Kitamura, T. et al. Engrams and circuits crucial for systems consolidation of a memory. *Science* **356**, 73–78 (2017).
3. Pernía-Andrade, A. J. & Jonas, P. Theta-gamma-modulated synaptic currents in hippocampal granule cells *in vivo* define a mechanism for network oscillations. *Neuron* **81**, 140–152 (2014).
4. Chawla, M. K. et al. Sparse, environmentally selective expression of Arc RNA in the upper blade of the rodent fascia dentata by brief spatial experience. *Hippocampus* **15**, 579–586 (2005).
5. Nakashiba, T. et al. Young dentate granule cells mediate pattern separation, whereas old granule cells facilitate pattern completion. *Cell* **149**, 188–201 (2012).
6. Danielson, N. B. et al. Distinct contribution of adult-born hippocampal granule cells to context encoding. *Neuron* **90**, 101–112 (2016).
7. Rubin, A., Geva, N., Sheintuch, L. & Ziv, Y. Hippocampal ensemble dynamics timestamp events in long-term memory. *eLife* **4**, e12247 (2015).
8. Mankin, E. A. et al. Neuronal code for extended time in the hippocampus. *Proc. Natl Acad. Sci. USA* **109**, 19462–19467 (2012).
9. Kentros, C. G., Agnihotri, N. T., Streater, S., Hawkins, R. D. & Kandel, E. R. Increased attention to spatial context increases both place field stability and spatial memory. *Neuron* **42**, 283–295 (2004).
10. Mankin, E. A., Diehl, G. W., Sparks, F. T., Leutgeb, S. & Leutgeb, J. K. Hippocampal CA2 activity patterns change over time to a larger extent than between spatial contexts. *Neuron* **85**, 190–201 (2015).
11. GoodSmith, D. et al. Spatial representations of granule cells and mossy cells of the dentate gyrus. *Neuron* **93**, 677–690.e5 (2017).
12. Senzai, Y. & Buzsáki, G. Physiological properties and behavioral correlates of hippocampal granule cells and mossy cells. *Neuron* **93**, 691–704.e5 (2017).
13. Sheffield, M. E. J., Adoff, M. D. & Dombeck, D. A. Increased prevalence of calcium transients across the dendritic arbor during place field formation. *Neuron* **96**, 490–504.e5 (2017).
14. Rajasethupathy, P. et al. Projections from neocortex mediate top-down control of memory retrieval. *Nature* **526**, 653–659 (2015).
15. Nitz, D. & McNaughton, B. Differential modulation of CA1 and dentate gyrus interneurons during exploration of novel environments. *J. Neurophysiol.* **91**, 863–872 (2004).
16. Leutgeb, J. K., Leutgeb, S., Moser, M.-B. & Moser, E. I. Pattern separation in the dentate gyrus and CA3 of the hippocampus. *Science* **315**, 961–966 (2007).
17. Diamantaki, M., Frey, M., Berens, P., Preston-Ferrer, P. & Burgalossi, A. Sparse activity of identified dentate granule cells during spatial exploration. *eLife* **5**, e20252 (2016).
18. Burgalossi, A., von Heimendahl, M. & Brecht, M. Deep layer neurons in the rat medial entorhinal cortex fire sparsely irrespective of spatial novelty. *Front. Neural Circuits* **8**, 74 (2014).
19. Stefanelli, T., Bertollini, C., Lüscher, C., Muller, D. & Mendez, P. Hippocampal somatostatin interneurons control the size of neuronal memory ensembles. *Neuron* **89**, 1074–1085 (2016).
20. Lee, S.-H. et al. Parvalbumin-positive basket cells differentiate among hippocampal pyramidal cells. *Neuron* **82**, 1129–1144 (2014).
21. Cai, D. J. et al. A shared neural ensemble links distinct contextual memories encoded close in time. *Nature* **534**, 115–118 (2016).
22. Driscoll, L. N., Pettit, N. L., Minderer, M., Chettih, S. N. & Harvey, C. D. Dynamic reorganization of neuronal activity patterns in parietal cortex. *Cell* **170**, 986–999.e16 (2017).
23. Tsao, A. et al. Integrating time in the entorhinal cortex. In *Society for Neuroscience* 084.21.2017 (2017).
24. Bittner, K. C., Milstein, A. D., Grienberger, C., Romani, S. & Magee, J. C. Behavioral time scale synaptic plasticity underlies CA1 place fields. *Science* **357**, 1033–1036 (2017).
25. Peters, A. J., Chen, S. X. & Komiyama, T. Emergence of reproducible spatiotemporal activity during motor learning. *Nature* **510**, 263–267 (2014).
26. Brandalise, F. & Gerber, U. Mossy fiber-evoked subthreshold responses induce timing-dependent plasticity at hippocampal CA3 recurrent synapses. *Proc. Natl Acad. Sci. USA* **111**, 4303–4308 (2014).

27. Roy, D. S. et al. Memory retrieval by activating engram cells in mouse models of early Alzheimer's disease. *Nature* **531**, 508–512 (2016).
28. Bernier, B. E. et al. Dentate gyrus contributes to retrieval as well as encoding: evidence from context fear conditioning, recall, and extinction. *J. Neurosci.* **37**, 6359–6371 (2017).
29. van Groen, T., Miettinen, P. & Kadish, I. The entorhinal cortex of the mouse: organization of the projection to the hippocampal formation. *Hippocampus* **13**, 133–149 (2003).
30. Kheirbek, M. A. et al. Differential control of learning and anxiety along the dorsoventral axis of the dentate gyrus. *Neuron* **77**, 955–968 (2013).

Acknowledgements We thank H.-J. Weber, C. Paun and C. Schmidt-Hieber for advice and help with setting up the virtual environment system; K. Winterhalter and K. Semmler for technical support; and J. Sauer, M. Strueber and M. Eyre for comments on earlier versions of the manuscript. This work was funded by the German Research Foundation (FOR2143, M.B.) and ERC-AdG 787450 (M.B.). This work was supported in part by the Excellence Initiative of the German Research Foundation (GSC-4, Spemann Graduate School; T.H.).

Reviewer information *Nature* thanks M. Brecht and S. Leutgeb for their contribution to the peer review of this work.

Author contributions T.H. and M.B. conceived the study, designed the experiments and wrote the manuscript. T.H. performed experiments and analysed data.

Competing interests The authors declare no competing interests.

Additional information
Extended data is available for this paper at https://doi.org/10.1038/s41586-018-0191-2.
Supplementary information is available for this paper at https://doi.org/10.1038/s41586-018-0191-2.

Correspondence and requests for materials should be addressed to M.B.